



**Immobilized CdS Quantum Dots in Spherical Polyelectrolyte  
Brushes: Fabrication, Characterization and Optical  
Properties**

Journal:	<i>Journal of Materials Chemistry C</i>
Manuscript ID:	TC-ART-10-2014-002456.R2
Article Type:	Paper
Date Submitted by the Author:	04-Feb-2015
Complete List of Authors:	<p>Cang, Yu; East China University of Science and Technology, State-Key Laboratory of Chemical Engineering  Zhang, Rui; East China University of Science and Technology, State-Key Laboratory of Chemical Engineering  shi, guixin; East China University of Science and Technology,  Zhang, Jianchao; East China University Science and Technology, State-Key Laboratory of Chemical Engineering  Liu, Lixiao; East China University Science and Technology, State-Key Laboratory of Chemical Engineering  Hou, Xiaoyan; East China University of Science and Technology, State-Key Laboratory of Chemical Engineering  Yu, Zhenchuan; East China University of Science and Technology, State-Key Laboratory of Chemical Engineering  Fang, Dingye; East China University of Science and Technology, State-Key Laboratory of Chemical Engineering  Guo, Xuhong; East China University of Science and Technology, State-Key Laboratory of Chemical Engineering</p>

## ARTICLE

# Immobilized CdS Quantum Dots in Spherical Polyelectrolyte Brushes: Fabrication, Characterization and Optical Properties

Cite this: DOI: 10.1039/x0xx00000x

Yu Cang, Rui Zhang\*, Guixin Shi, Jianchao Zhang, Lixiao Liu, Xiaoyan Hou, Zhenchuan Yu, Dingye Fang, Xuhong Guo\*

Received 00th January 2012,

Accepted 00th January 2012

DOI: 10.1039/x0xx00000x

[www.rsc.org/](http://www.rsc.org/)

In this work, we demonstrated a facile and environmental-friendly method of preparing water-soluble cadmium sulfide (CdS) quantum dots (QDs) immobilized in spherical polyelectrolyte brushes (SPBs). The synthesis included three stages as following: preparation of SPBs, introduction of Cd<sup>2+</sup> by ion-exchange process and in-situ fabrication of CdS in SPBs. X-ray diffraction (XRD) pattern and the transmission electron microscope (TEM) images proved the CdS nanocrystallines (NCs) were cubic structure and well distributed in SPBs. The size and photoluminescence (PL) emission of hybrid nanoparticles (SPBs@CdS) could be tailored by adjusting some parameters, such as pH of SPBs, ratio of Cd/S, temperature of reaction and dimension of SPBs@CdS. For instance, increasing pH of SPBs and the ratio of Cd/S, the trap emission of CdS NCs could be transferred to band-edge emission. And the PL emission shifted from 490 to 580 nm as reaction temperature increased from 10 to 90 °C. More interesting was that the PL emission of SPBs@CdS could be quenched and recovered reversibly by pH adjustment due to the pH sensitive chains of poly(acrylic acid) grafting from polystyrene core. The SPBs@CdS displayed excellent photochemical stability in visible light above pH 10 which provided a possibility for storage QDs in visible light. In addition, this simple method can be extended to other sulfide fabrication in SPBs, such as ZnS, which also been successfully embedded in SPBs.

## Introduction

Quantum Dots (QDs) attract multiple interests for modified optical and electronic properties during last 20 years. Comparing with traditional organic dyes, advantages of long lifetime, broad excitation range, good photochemical stability and high fluorescence intensity make QDs suitable in applications of biodiagnostics, bioimaging, photonics, solar cell and sensors. As an important member of II-VI groups QDs, CdS nanocrystallines (NCs), with band edge energy of 2.42 eV, are attractive for absorbing visible light in the solar spectrum. Obtaining high-quality QDs was a bottleneck in this field until organometallic routes were firstly developed by Murray et al<sup>1</sup>. Then other alternatives, such as long chain amine and carboxylic acid<sup>2, 3</sup>, were adopted to cap the surface of nanoparticles and well developed. However, the pyrolysis of organometallic reagents is toxic and harmful for environment and the hydrophobicity hinder the biological applications of QDs. So it is necessary to change the hydrophobic character and transfer QDs to aqueous for biology fields.

Replacing hydrophobic capping ligands by hydrophilic or bifunctional ligands is one way to transfer QDs from nonpolar medium to aqueous solution. But the electronic or optical properties may be deteriorated during this process and the proper selection of ligands has limitations. Many strategies are developed to acquire high quality water-soluble QDs, including (i) coating the surface of QDs with polymers<sup>4, 5</sup>, (ii) polymerization of monomers in presence of QDs and (iii) synthesis of QDs in polymers. For the first method, there are many kinds of polymers reported to be attached to the surface of QDs, such as amphiphilic copolymers<sup>6</sup>, multidentate polymeric ligands<sup>7-9</sup> and dendrimer<sup>10, 11</sup>. But these approaches usually contain several steps and the design of polymers or monomers is still a challenge. The second method, polymerization in the presence of QDs, is usually encapsulating QDs in polymer cores that give QDs to aqueous solution<sup>12, 13</sup>. This method could prevent the aggregation and phase separation of QDs. But homogeneous distribution of QDs in the polymer cores is not easy and some of QDs are apt to be attracted on the surface of nanoparticles<sup>14</sup>. In addition, the prepared QDs are usually TOPO-coated of which preparation is

not environmental-friendly. Therefore, generation of QDs in water-soluble polymers is a good option, which is low-cost, relatively green to environment and easily handling. Zeolite<sup>15</sup>, polymer blend<sup>16, 17</sup> and nafion film<sup>18</sup> have been used as templates for QDs generation. Hybrid polymer-QDs nanoparticles exhibit optical property, good photochemical stability and water solubility<sup>17, 19, 20</sup>. But the optical characteristic is not easily tuneable and the stimulate-responsive properties of polymers may be lost.

SPBs are systems with functional polymer chains densely grafting from latex particles<sup>21</sup>. Dispersing in water and carrying high charges, SPBs have been successfully loaded with noble metals of Au, Pt and Ni which display high catalytic activity on reduction of p-nitrophenol<sup>22-24</sup>. Besides, SPBs are ideal candidates for protein carriers and separation, drug delivery, high-performance diagnostic assay.<sup>25-27</sup> High stability and stimuli-sensitivity make SPBs suitable nanoreactors for formation of QDs. Brushlike chains are idea QDs carriers and the high grafting density of polymer chains could assist introduction of ions and enhance the capacity of immobilization<sup>28-31</sup>. Therefore, SPBs should be promising candidates for QDs immobilization.

In this work, we in-situ generated CdS in SPBs with high quality under normal pressure. The surface state and PL emission of CdS QDs could be modified by adjustment of pH values due to the pH sensitive property of PAA chains. Following swollen and shrinkage of SPBs, the PL emission could be quenched and recovered with little loss. The hybrid nanoparticles exhibited high photochemical stability under visible light. Besides, this method could also be extended to synthesize other sulphide such as ZnS in the SPBs.

## Experiment section

### Materials

All the chemical used for experiment are analytical grade as received. Styrene (Shanghai reagent company (SRC)) and acrylic acid (AA) (SRC) were distilled under reduced pressure and stored at 4 °C until used. Potassium persulfate (KPS) (J&K Chemical) was used as initiator and sodium dodecyl sulfonate (SDS) (J&K Chemical) was used as surfactant in synthesis of polymer core. Cadmium chloride hemi(pentahydrate) ( $\text{CdCl}_2 \cdot 2.5\text{H}_2\text{O}$ ) (Aladdin), Zinc chloride ( $\text{ZnCl}_2$ ) (SRC), Sodium hydroxide (NaOH) (SRC) and Sodium sulfide nonahydrate ( $\text{Na}_2\text{S} \cdot 9\text{H}_2\text{O}$ ) (SRC) was used as received. The water used in all experiments was purified by reverse osmosis (Shanghai RO Micro Q).

### Synthetic procedures

#### SYNTHESIS OF POLYSTYRENE (PS) CORE

The emulsion polymerization method was used for synthesis of polystyrene core. The mixture of styrene (2 g), SDS (0.1 g) and KPS (0.03 g) in 50 ml  $\text{H}_2\text{O}$  was heated at 80°C under nitrogen atmosphere. As stirring for one hour, the photoinitiator 2-[p-(2-hydroxy-2-methylpropiophenone)]-ethyleneglycol methacrylate (HMEM, 0.2 g) (synthesis in our laboratory) dissolved in acetone (1 g) was added into mixture in 10 min under starved condition. Then further reacted for one hour, the PS core with thin layer of HMEM was obtained. The latex was purified by dialysis against water until the conductivity of water was reduced to  $2 \mu\text{S} \cdot \text{cm}^{-1}$ .

#### SYNTHESIS OF SPBS

Adding AA monomer (75 wt% relative to mass of PS cores in dry state) to the latex of PS@HMEM with weight content of 1 wt%, the mixture was moved to a homemade UV-reactor (range of wavelengths: 200-600 nm, power: 150 W) and exposed in the UV light for 60min, which was photoemulsion polymerization. The obtained SPBs was dialyzed and stored under room temperature.

#### PREPARATION OF CDS QUANTUM DOTS IN SPBS

The pH of SPBs solution was adjusted to a required values by NaOH solution ( $0.1 \text{ mol} \cdot \text{L}^{-1}$ ). A amount of  $\text{CdCl}_2 \cdot 2.5\text{H}_2\text{O}$  (1 mmol of metal salt per gram of SPBs) was added into SPBs solution and the dispersion was stirring for overnight to fully ion-exchange between  $\text{Na}^+$  and  $\text{Cd}^{2+}$  ions. Then the mixture was then dialyzed to remove free  $\text{Cd}^{2+}$  ions outer SPBs layers. Following this step, a 0.01 M  $\text{Na}_2\text{S}$  solution was adding into dispersion by droplet under  $\text{N}_2$  protection. Once the  $\text{S}^{2-}$  ions introduced in dispersion, the colour immediately turned to slight yellow and become darker as increasing quantity of  $\text{Na}_2\text{S}$  which implied formation of CdS nanoparticles in SPBs. The dispersion was stirring for 2 h and stored in dark place.

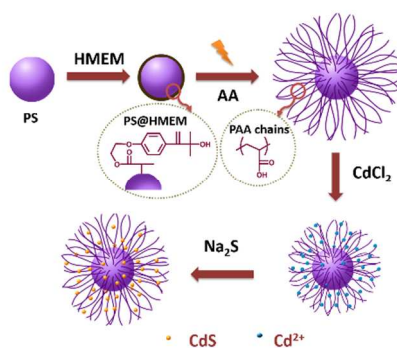
#### Characterization methods

The hydrodynamic size of particles was determined by dynamic light scattering (DLS) which was performed by a particle sizing system of NICOMP 380 ZLS at a fixed scattering angle of 90°. UV-vis and PL spectra were obtained on a Shimadzu UV-2550 spectrometer and Cary Eclipse (Varian) fluorometer, respectively. Transmission electron micrographs (TEM) were taken on a JEOL JEM-2100F at an acceleration voltage at 200 kV. The SPBs@CdS solution was diluted to 0.01 wt% and then dropped on 300 mesh carbon-coated copper grid. The excess solution was carefully removed with filter paper. The TEM grid was dried under infrared light for a few minutes before carried on TEM test. X-Ray powder diffraction (XRD) was measured by wide-angle X-ray scattering, using a Bruker D8 Advance diffractometer equipped with graphite monochromated high-intensity Cu-K $\alpha$  radiation ( $\lambda = 1.5418 \text{ \AA}$ ). XRD samples were prepared by depositing NC powder on a piece of Si (100)

wafer. The pH value of a solution was measured by a PHS-3C pH meter.

## Results and discussion

The synthesis process of SPBs@CdS included three steps: preparation of SPBs, ion-exchange process and in-situ formation of CdS QDs as shown in scheme 1. In the first stage, the SPBs were prepared by photoemulsion polymerization which has been detailed in the previous literature<sup>21</sup>. The diameter of PS core and SPBs (at pH 8) was ~90 nm and ~620 nm respectively which were monitored by DLS as shown in Figure S1. (Supporting Information) In the second stage, Cd<sup>2+</sup> ions were introduced into brush layers by ion-exchange process between deprotonated carboxylic acid groups and water-soluble salt. The diameter of SPBs decreased from ~620 (at pH 8) to ~350 nm due to the introduction of divalent ions. (Figure S1) Then, the CdS NCs were formed as dropwisely addition of Na<sub>2</sub>S solution into SPBs@Cd<sup>2+</sup>, confirmed by a change in the colour of solution from opal to yellow. Meanwhile, the size of SPBs@CdS increased to ~405 nm for consumption of Cd<sup>2+</sup> ions which was a cue of CdS formation<sup>24</sup>. (Figure S1) Using Na<sub>2</sub>S as precipitant, the S<sup>2-</sup> ions entered into the system very fast which was a drawback to give small size of particles. Therefore, controlling the dropping speed of Na<sub>2</sub>S was crucial for QDs formation and distribution. Centrifuging the SPBs@CdS solution, there was no precipitate indicating CdS NCs were firmly confined within layers of SPBs. The whole synthesis process was carried out under room temperature without any toxic organic solvent assisted and ligand exchange step. Compared with hydrothermal method and solvothermal method, it was convenient, non-toxic and environment-friendly.



Scheme 1 Preparation of SPBs@CdS

Ionic strength was an important parameter for dimension of SPBs controlling. The salt ions could screen electronic repulsion between carboxylic acid groups that contracted polymer chains. The divalent ions show stronger effect on shrinkage of SPBs than that of monovalent ions.<sup>24, 32</sup> At high ionic strength, the “salting-in” effect could dramatically reswell brush layers that leads to flocculation<sup>33</sup>. So the concentration of Cd<sup>2+</sup> ions should be limited avoiding aggregation of SPBs.

Table 1 showed diameter of SPBs with different weight content (0.1 wt%, 0.05 wt%, 0.01 wt%) at different concentration of CdCl<sub>2</sub>. It was interesting to find that the diameter of SPBs@Cd<sup>2+</sup> depended on the mole of Cd<sup>2+</sup> per gram of SPBs ( $n_{\text{CdCl}_2}/m_{\text{SPBs}}$ ) rather than the concentration of Cd<sup>2+</sup>.<sup>24</sup> At  $n_{\text{CdCl}_2}/m_{\text{SPBs}}$  1, the size of SPBs was reduced by about 260 nm and the polydispersity index (PI) was ~0.050 which suggested the SPBs were still monodispersed in the solution. As  $n_{\text{CdCl}_2}/m_{\text{SPBs}}$  increased to 2, the PI sharply increased to ~0.280, indicating the SPBs were not stable and inclined to flocculate. The SPBs were completely aggregated at  $n_{\text{CdCl}_2}/m_{\text{SPBs}}$  4. Therefore, we selected  $n_{\text{CdCl}_2}/m_{\text{SPBs}}$  1 (highlight in table 1) in the following experiments.

Table 1 Diameter of SPBs (0.1 wt%, 0.05 wt%, 0.01 wt%) under different  $n_{\text{CdCl}_2}/m_{\text{SPBs}}$ . The samples were tested at pH 8.

$n_{\text{CdCl}_2}/m_{\text{SPBs}}$ (mmol/g)	0.1 wt%		0.05 wt%		0.01 wt%	
	D (nm)	PI	D (nm)	PI	D (nm)	PI
0	602	0.031	618	0.028	621	0.023
1	345	0.088	355	0.051	367	0.045
2	161	0.343	178	0.283	206	0.243
4	Aggregation		Aggregation		Aggregation	

$n_{\text{CdCl}_2}/m_{\text{SPBs}}$ : the ratio of mole of CdCl<sub>2</sub> per gram of SPBs

### 3.1 Effect of weight content of SPBs@CdS.

Fig. 1 showed UV-vis and PL spectra of SPBs@CdS (0.1 wt%, 0.05 wt%, 0.01 wt% of SPBs). All three samples had a blue shift of absorption peak at about 410 nm, compared with bulk CdS at 515 nm (2.4 eV) in Fig. 1 (A). The absorption peak was at ~405, 413 and 417 nm for 0.01 wt%, 0.05 wt% and 0.1 wt% SPBs@CdS respectively. The shorter wavelength indicated formation of smaller-sized CdS NCs in the 0.01 wt% SPBs. The PL peak of three samples was at ~570 nm in Fig. 1 (B) which was associated with recombination of electron trapped in a sulfur vacancy and a hole in the valence band of CdS.<sup>17, 34, 35</sup> The surface defects, which broadened PL spectra and deteriorated the relation between size of QDs and band-gap emission, were common to observe in aqueous preparation for their high surface-to-volume ratio.<sup>36, 37</sup> The 0.05 wt% SPBs@CdS demonstrated highest PL peak which was eight times than that of 0.1 wt% SPBs@CdS. It was ascribed to the low weight content of Cd of SPBs and concentration of Cd<sup>2+</sup>. With high weight content of SPBs, the 0.1 wt% SPBs solution were opaque and had high refractive index. It tended to scatter more photons reached the surfaces of QDs to be excited. To investigate which reason played a dominant role, we decreased the concentration of Cd<sup>2+</sup> ions in 0.1 wt% SPBs. (Figure S2, In Supporting Information) The slightly improvement of PL intensity implied that the high weight content of SPBs was the main reason for low PL emission of SPBs@CdS. So we used 0.01 wt% SPBs in the following experiments to investigate the effects of other parameters on the quality of QDs.

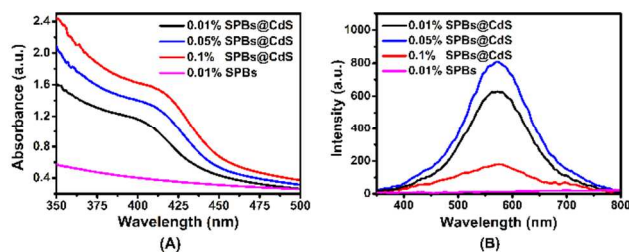


Fig. 1 UV-vis (A) and PL spectra (B) ( $\lambda_{\text{exc}}=360$  nm) of SPBs@CdS with different weight concentration.  $[\text{Cd}^{2+}]:[\text{S}^{2-}]=1:1.5$ ,  $T=30$  °C.

### 3.2 Effect of ratio of S/Cd on SPBs@CdS.

The elements terminated on the surface of CdS QDs significantly affect their passivation of traps and PL emission. The band-edge emission of CdS QDs could be quenched by S termination on the surface and recovered again by capping Cd element as reported by Krauss et al.<sup>38</sup>. Therefore, the ratio of S/Cd is important for the modification of surface states. The PL spectra and zeta potential of SPBs@CdS with different ratio of S/Cd were illustrated in Fig. 2 (A) and (B) respectively. In Fig. 2 (A), the band-edge emission was at  $\sim 450$  nm and a small trap edge emission appeared at  $\sim 572$  nm as S/Cd was 0.8. The strong band-edge emission indicated the passivation of surface defects of NCs. As the ratio of S/Cd increased to 1.0, the band-edge emission decreased by half while the trap emission was highly enhanced by six times comparing with that of SPBs@CdS with S/Cd 0.8. The red shift of band-edge emission indicated the CdS NCs were still growing. The band-edge emission was completely quenched at S/Cd 1.5 due to numerous surface defects introduction into CdS NCs. It was also supported by zeta potential of hybrid nanoparticles in Fig. 2 (B). The decrease of band-edge emission agreed with decrease of zeta potential which was related to the surface charges of nanoparticles<sup>39, 40</sup>. At S/Cd 0.8, the large zeta potential of SPBs@CdS suggested cations were enriched on the surface of particles<sup>41, 42</sup>. It probably due to  $\text{Cd}^{2+}$  terminated on the CdS NCs which was contributed to high band-edge emission. As increasing of S/Cd above 1.5, the CdS NCs continued grow and adsorbed  $\text{S}^{2-}$  ions on the surface that led to decrease of zeta potential below  $\sim 60$  mV. The S termination of CdS QDs brought effective nonradiative recombination and caused the decrease of band-edge emission.<sup>38</sup> The small enhancement of zeta potential may be due to the compensation by some  $\text{Na}^+$  ions at S/Cd 2.0.

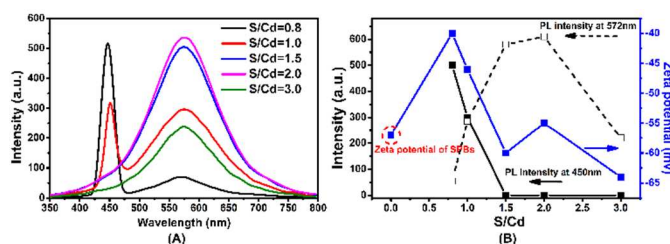


Fig. 2 (A) The PL spectra of SPBs@CdS at different ratio of S/Cd. (B) Zeta potential of SPBs@CdS (blue square), PL intensity at 450 nm (black square) and 572 nm (white hollow square) under different ratio of S/Cd.

### 3.3 Effect of temperature on PL intensity

Fig. 3 displayed UV-vis and PL spectra of SPBs@CdS synthesized at different temperature. As temperature increased from 10 to 90 °C, the absorbance peak had red-shift from  $\sim 380$  to  $\sim 450$  nm in Fig. 3 (A) which indicated the formation of big-sized NCs at high temperature, because the low temperature was benefit to reduce crystal growing rate that decrease the size of particles<sup>24</sup>. According to the following formula (1)<sup>43, 44</sup>, the average diameter of CdS QDs was ranged from 2.82 to 5.27 nm. The TEM images and size distribution of CdS QDs synthesized at 10, 50, 90 °C were shown in Figure S3. (In supporting information)

$$D = \left( -6.6521 \times 10^{-8} \right) \lambda^3 + \left( 1.9557 \times 10^{-4} \right) \lambda^2 - \left( 9.2352 \times 10^{-2} \right) \lambda + 13.29 \quad (1)$$

The normalized fluorescence spectra of CdS QDs exhibited red-shift from  $\sim 490$  to  $\sim 580$  nm with temperature increase in Fig. 3 (B). This particle-size-dependent trap-state was also mentioned by Shih<sup>45</sup>. The emission of SPBs@CdS could be tuned from green to yellow by reaction temperature, which provided an alternate way of using continuously trap emission in optical devices and fluorescence probes.

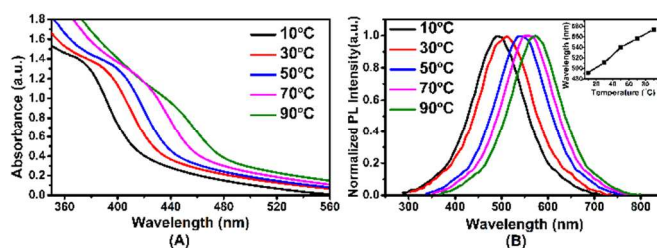


Fig. 3 UV-vis spectra (A) and PL spectra (B) of SPBs@CdS synthesized at different temperature.

### 3.4 Effect of precursor pH

Fig. 4 (A) shows the PL spectra of SPBs@CdS with different pH (5, 7, 9, 10, 11) of precursor of SPBs. In neutral and base solution, the narrow band-edge emission appeared at 450 nm and increased with pH of SPBs. The trap emission decreased and shifted to shorter wavelength. It was probably caused by the formation of  $\text{Cd}(\text{OH})_2$  shell outside the CdS QDs which could passive the surface defects<sup>46</sup>. At pH 5, the band-edge emission were quenched and replaced by trap emission peak at  $\sim 570$  nm. Diameter of SPBs, band-edge emission intensity and weight content of CdS QDs with pH of SPBs were displayed in Fig. 4 (B). The three lines displayed similar trend, which increased with pH values. At high pH values, the ionized PAA chains were fully stretched and had multi nucleation sites for complexation with  $\text{Cd}^{2+}$  ions. The weight content of CdS reached to 35 wt.-% at pH 9, while only 15 wt.-% at pH 5. Although the

PAA chains can provide multiple bonding sites to coordinate with  $\text{Cd}^{2+}$  ions at lower pH<sup>47,48</sup>, the shrinkage of layers limited the immobilization of CdS NCs and led to weak PL emission at low pH values. The two factors of the ionized PAA chains and swollen shell were interdependent and difficult to investigate separately. Therefore, which one was prominent or both of them were significant was unclear.

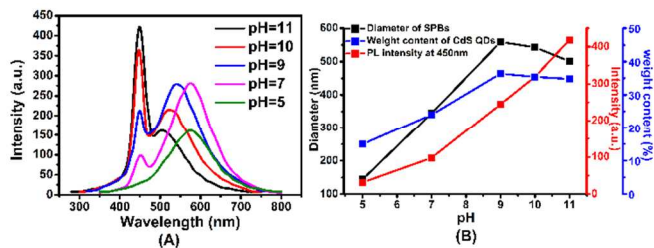


Fig. 4 (A) The PL spectra of SPBs@CdS with different pH values of precursor. (B) Diameter of SPBs (black square), PL intensity of SPBs@CdS at 450 nm (red square), weight content of CdS QDs (blue square) at different pH values of precursor.

### 3.5 Response of SPBs@CdS to pH adjustment

The PL intensity and diameter of SPBs@CdS with different pH was shown in Fig. 5 (A). The tendency of two lines are similar that increased with pH values and then slightly decreased above pH 10. Below pH 5, the SPBs@CdS was shrunken and the PL emission was almost quenched. There were two reasons for low PL intensity at acid condition. One was that the coil polymer chains would wrap on the surface of CdS QDs and scatter many photons to reach the surface of CdS QDs. The other was the close packing structure of CdS QDs which was also seen in other papers<sup>49, 50</sup>. Increasing pH from 5 to 8, the length of polymer chains was doubled and PL intensity was enhanced by a factor of 4. The formation of  $\text{Cd}(\text{OH})_2$  shell played a key role in the increment of PL intensity. This thin shell could passive the surface defects of QDs and confine the wave function of electro-hole pairs in the interior of the nanocrystals which led to reduction of the non-radiation relaxation at surface sites and surface traps<sup>51</sup>. Above pH 10, the slight decrease of diameter was caused by “salt screening” effect<sup>52</sup> accompanying by reduction of PL emission. It should be noted that the variation of PL emission was reversible by adjusting pH of SPBs@CdS. Increasing the pH from 3 to 10, the PL emission can be recovered with slight loss in Figure S4. Fig. 5 (B) showed the PL intensity comparison of as prepared SPBs@CdS with that exposure in visible light for 60 days. The PL intensity of SPBs@CdS sharply decreased below pH 9 after long time exposure in visible light. While the SPBs@CdS exhibited excellent photochemical stability above pH 10 especially at pH 12 due to the protection of  $\text{Cd}(\text{OH})_2$  shell,<sup>51</sup> which provided a method for storage of QDs in visible light. Stored in the dark, all the samples had slight PL loss. Different with thiol-capped QDs<sup>53, 54</sup>, there was no aggregation in the solution, which was

the reason for PL emission loss of thiol-capped QDs, indicating the high stability of SPBs@CdS.

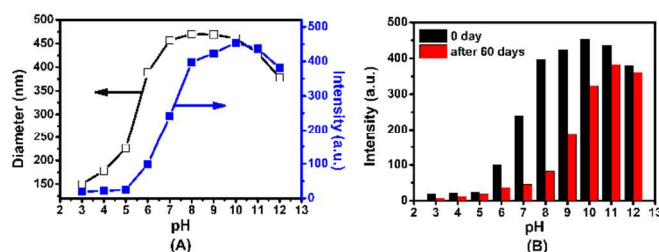


Figure 5. (A) The diameter and PL intensity of 0.01% SPBs@CdS at 450nm with different pH values. (B) The PL intensity comparison 0.01% SPBs@CdS exposed under visible light with 0 and 60 days

Fig. 6 (A), (B), (C) showed TEM and HRTEM images of SPBs@CdS synthesized at 30 °C. In Fig. 6 (A) and (B), the diameter of PS core was about ~90 nm which was coincided with DLS analysis. The CdS QDs were successfully immobilized in the SPBs with narrow distribution. Enlarging SPBs@CdS with high resolution in Fig. 6 (B), the diameter of CdS QDs was below 4 nm and fully crystalline. Fig. 6 (D) displayed the average diameter of CdS NCs was about ~2.8 nm.

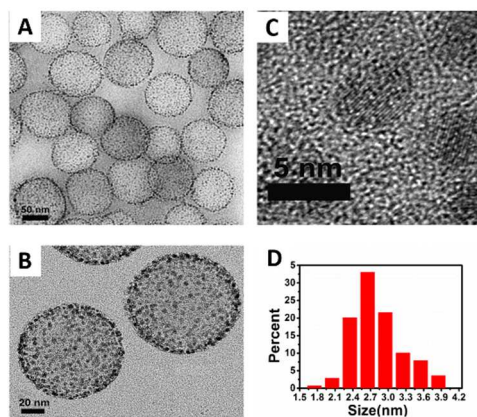


Fig. 6 (A), (B), (C) TEM and HRTEM photos of SPBs@CdS hybrid nanoparticles. (D) Size distribution of the SPBs@CdS counted from (A), (B)

XRD pattern was illustrated in Fig. 7 to identify the structure of CdS NCs, which was obtained from pattern of SPBs and SPBs@CdS in Figure S5. The reflection peak at scattering angles ( $2\theta$ ) of CdS was 26.6, 43.7, 52.1, respectively which was corresponded to scattering from the (111), (220) and (311) planes. The pattern was well fitted with cubic phase (JCPDS no. 10-0454).

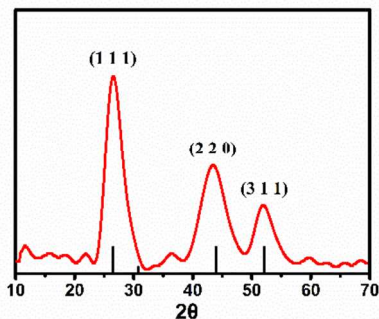


Fig. 7 XRD pattern of CdS.

This method could be applied to synthesis of other sulfide such as ZnS. Fig. 8 showed the TEM and HRTEM images of SPBs@ZnS. In Fig. 8 (A), (B), (D), we can see the ZnS QDs were well dispersed in SPBs with diameter about  $\sim 3$  nm. In Fig. 8 (C), the HRTEM photos showed the crystalline structure of ZnS. Both SPBs@CdS and SPBs@ZnS can be stored over six months without flocculation.

As described above, Both CdS and ZnS NCs can be generated in brush layers and display tuneable optical property. By ion-exchange process, the  $\text{Cd}^{2+}$  ions interacted with  $\text{COO}^-$  and formed Cd-carboxylic complex within layers of SPBs. Dropwisely adding  $\text{S}^{2-}$  ions into solution, a large number of nucleus was formed and the growth process was kinetically controlled, which was usually formed cubic polycrystalline.<sup>55,56</sup> The growth speed of QDs could be adjusted by temperature that gave hybrid nanoparticles with emission from green to yellow. Th synthesis of QDs was carried out under nitrogen atmosphere. Without passivation of oxygen on the non-polar facet, the nucleus grew into thickness and even spherical nanoparticles<sup>56</sup> which was proved by TEM images.

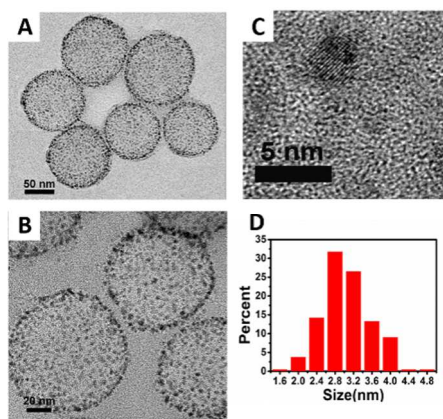


Fig. 8 (A), (B) (C) TEM and HRTEM photos of SPBs@ZnS prepared at 273 K. (D) Size distribution of the SPBs@ZnS counted from (A), (B)

## Conclusions

In this paper, CdS NCs have been firmly embedded in SPBs with narrow size-distribution. The hybrid nanoparticles exhibited size-dependence optical property because the diameter of CdS NCs, in the range of 2.8  $\sim$  5.3 nm, was below Bohr radius. By adjusting temperature, ratio of S/Cd and pH of SPBs, the emission spectra could be modified from green to yellow. Moreover, the PL emission could be reversibly quenched and recovered by alteration of the length of PAA chains. The SPBs@CdS performed good photochemical stability at high pH values in visible light. This synthesis method can be applied to preparation of other QDs in II-VI groups such as ZnS which has also been successfully embedded in SPBs. The water-soluble SPBs@QDs could be promising candidates in biology fields.

## Acknowledgements

This work is supported by National Natural Science Foundation of China (21004021, 21374029), the Fundamental Research Funds for the central universities (WA1014007, 222201313011), Shanghai Education Innovation Key Project (14ZZ061), State-Key Laboratory open subject SKL-ChE-11CO2, The start funding of East China University of Science and Technology YA0142119.

## Notes and references

State-Key Laboratory of Chemical Engineering, East China University of Science and Technology, Shanghai 200237, China  
E-mail: r.zhang@ecust.edu.cn, guoxuhong@ecust.edu.cn  
Electronic Supplementary Information (ESI) available:  
See DOI: 10.1039/b000000x/

1. C. B. Murray, D. J. Norris and M. G. Bawendi, *J Am Chem Soc*, 1993, 115, 8706-8715.
2. W. W. Yu and X. Peng, *Angewandte Chemie - International Edition*, 2002, 41, 2368-2371.
3. X. Zhong, S. Liu, Z. Zhang, L. Li, Z. Wei and W. Knoll, *J Mater Chem*, 2004, 14, 2790-2794.
4. R. M. Crooks, M. Zhao, L. Sun, V. Chechik and L. K. Yeung, *Accounts Chem Res*, 2000, 34, 181-190.
5. H. Skaff, K. Sill and T. Emrick, *J Am Chem Soc*, 2004, 126, 11322-11325.
6. C. Luccardini, C. Tribet, F. Vial, V. Marchi-Artzner and M. Dahan, *Langmuir*, 2006, 22, 2304-2310.
7. I. Potapova, R. Mruk, C. Hübner, R. Zentel, T. Basché and A. Mews, *Angewandte Chemie International Edition*, 2005, 44, 2437-2440.
8. D. Zhou, Y. Li, E. A. H. Hall, C. Abell and D. Klenerman, *Nanoscale*, 2011, 3, 201-211.
9. C. Querner, P. Reiss, J. Bleuse and A. Pron, *J Am Chem Soc*, 2004, 126, 11574-11582.
10. T. Nann, *Chem Commun*, 2005, 1735-1736.
11. X. C. Wu, A. M. Bittner and K. Kern, *The Journal of Physical Chemistry B*, 2004, 109, 230-239.

12. A. Esteves, A. Barros-Timmons, I. Monteiro and T. Trindade, *J Nanosci Nanotechnol*, 2005, 5, 766-771.
13. N. Joumaa, M. Lansalot, A. Th  retz, A. Elaissari, A. Sukhanova, M. Artemyev, I. Nabiev and J. H. M. Cohen, *Langmuir*, 2006, 22, 1810-1816.
14. S. V. Vaidya, M. L. Gilchrist, C. Maldarelli and A. Couzis, *Anal Chem*, 2007, 79, 8520-8530.
15. H. S. Kim, N. C. Jeong and K. B. Yoon, *J Am Chem Soc*, 2011, 133, 1642-1645.
16. J. Zhang, N. Coombs and E. Kumacheva, *J Am Chem Soc*, 2002, 124, 14512-14513.
17. J. Zhang, S. Xu and E. Kumacheva, *J Am Chem Soc*, 2004, 126, 7908-7914.
18. S. Wang, P. Liu, X. Wang and X. Fu, *Langmuir*, 2005, 21, 11969-11973.
19. J. Zhang, N. Coombs, E. Kumacheva, Y. Lin and E. H. Sargent, *Adv Mater*, 2002, 14, 1756-1759.
20. H. Du, G. Q. Xu, W. S. Chin, L. Huang and W. Ji, *Chem Mater*, 2002, 14, 4473-4479.
21. X. Guo, A. Weiss and M. Ballauff, *Macromolecules*, 1999, 32, 6043-6046.
22. G. Sharma and M. Ballauff, *Macromol Rapid Comm*, 2004, 25, 547-552.
23. Y. Mei, G. Sharma, Y. Lu, M. Ballauff, M. Drechsler, T. Irrgang and R. Kempe, *Langmuir*, 2005, 21, 12229-12234.
24. Z. Zhu, X. Guo, S. Wu, R. Zhang, J. Wang and L. Li, *Ind Eng Chem Res*, 2011, 50, 13848-13853.
25. N. Welsch, A. L. Becker, J. Dzubiella and M. Ballauff, *Soft Matter*, 2012, 8, 1428.
26. N. Welsch, A. Wittemann and M. Ballauff, *The Journal of Physical Chemistry B*, 2009, 113, 16039-16045.
27. S. Wang, K. Chen, Y. Xu, X. Yu, W. Wang, L. Li and X. Guo, *Soft Matter*, 2013, 9, 11276-11287.
28. G. Qian, B. Zhu, Y. Wang, S. Deng and A. Hu, *Macromol Rapid Comm*, 2012, 33, 1393-1398.
29. J. Yan, Q. Ye and F. Zhou, *RSC Advances*, 2012, 2, 3978-3985.
30. J. Yan, Q. Ye, X. Wang, B. Yu and F. Zhou, *Nanoscale*, 2012, 4, 2109-2116.
31. L. Ionov, S. Sapra, A. Synytska, A. L. Rogach, M. Stamm and S. Diez, *Adv Mater*, 2006, 18, 1453-1457.
32. Y. Mei and M. Ballauff, *The European Physical Journal E*, 2005, 16, 341-349.
33. S. Wang, K. Chen, L. Li and X. Guo, *Biomacromolecules*, 2013, 14, 818-827.
34. J. Chrysochoos, *The Journal of Physical Chemistry*, 1992, 96, 2868-2873.
35. J. J. Ramsden, S. E. Webber and M. Graetzel, *The Journal of Physical Chemistry*, 1985, 89, 2740-2743.
36. L. Zou, Z. Fang, Z. Gu and X. Zhong, *J Lumin*, 2009, 129, 536-540.
37. N. Chestnoy, T. D. Harris, R. Hull and L. E. Brus, *The Journal of Physical Chemistry*, 1986, 90, 3393-3399.
38. H. H. Wei, C. M. Evans, B. D. Swartz, A. J. Neukirch, J. Young, O. V. Prezhdo and T. D. Krauss, *Nano Lett*, 2012, 12, 4465-4471.
39. V. Fischer, M. B. Bannwarth, G. Jakob, K. Landfester and R. Mu  oz-Espi, *The Journal of Physical Chemistry C*, 2013, 117, 5999-6005.
40. V. Fischer, I. Lieberwirth, G. Jakob, K. Landfester and R. Munoz-Espi, *Adv Funct Mater*, 2013, 23, 451-466.
41. M. D. Peterson, S. C. Jensen, D. J. Weinberg and E. A. Weiss, *ACS Nano*, 2014, 8, 2826-2837.
42. A. J. Morris-Cohen, M. T. Frederick, G. D. Lilly, E. A. McArthur and E. A. Weiss, *The Journal of Physical Chemistry Letters*, 2010, 1, 1078-1081.
43. W. W. Yu, L. Qu, W. Guo and X. Peng, *Chem Mater*, 2003, 15, 2854-2860.
44. Y. Mo, Y. Tang, F. Gao, J. Yang and Y. Zhang, *Ind Eng Chem Res*, 2012, 51, 5995-6000.
45. H. Li, W. Y. Shih and W. Shih, *Ind Eng Chem Res*, 2007, 46, 2013-2019.
46. L. Spanhel, M. Haase, H. Weller and A. Henglein, *J Am Chem Soc*, 1987, 109, 5649-5655.
47. I. G. Dance, M. L. Scudder and R. Secomb, *Inorg Chem*, 1983, 22, 1794-1797.
48. H. Zhang, Z. Zhou, B. Yang and M. Gao, *The Journal of Physical Chemistry B*, 2002, 107, 8-13.
49. H. Dou, W. Yang, K. Tao, W. Li and K. Sun, *Langmuir*, 2010, 26, 5022-5027.
50. C. B. Murray, M. G. Bawendi and C. R. Kagan, *Phys Rev B*, 1996, 54, 8633-8643.
51. J. Yang, D. Deng and J. Yu, *J Colloid Interf Sci*, 2013, 394, 55-62.
52. S. Wang, K. Chen, L. Li and X. Guo, *Biomacromolecules*, 2013, 14, 818-827.
53. V. V. Breus, C. D. Heyes and G. U. Nienhaus, *The Journal of Physical Chemistry C*, 2007, 111, 18589-18594.
54. J. Aldana, Y. A. Wang and X. Peng, *J Am Chem Soc*, 2001, 123, 8844-8850.
55. H. Chu, X. Li, G. Chen, W. Zhou, Y. Zhang, Z. Jin, J. Xu and Y. Li, *Cryst Growth Des*, 2005, 5, 1801-1806.
56. G. Zhang, P. He, X. Ma, Y. Kuang, J. Liu and X. Sun, *Inorg Chem*, 2012, 51, 1302-1308.

# Immobilized CdS Quantum Dots in Spherical Polyelectrolyte Brushes: Fabrication, Characterization and Optical Properties

Yu Cang, Rui Zhang\*, Guixin Shi, Jianchao Zhang, Lixiao Liu, Xiaoyan Hou, Zhenchuan Yu, Dingye Fang, Xuhong Guo\*

The SPBs@CdS nanoparticles exhibit controlled and reversible photoluminescence with pH as a trigger and strong photochemical stability in basic solution.

